PERKIN 2

An odd–even relationship which appears in the aggregation modes of ‘gemini’-type cholesterol-based gelators and their transcription into silica gel

Jong Hwa Jung and Seiji Shinkai *

Chemotransfiguration Project, Japan Science and Technology Corporation (JST),
2432 Aikawa, Kurume, Fukuoka 839-0861, Japan

Received (in Cambridge, UK) 7th July 2000, Accepted 11th September 2000
First published as an Advance Article on the web 6th November 2000

Four ‘gemini’-type cholesterol-based gelators $\mathbf{1}_n$ were synthesized. They acted as versatile gelators of organic fluids. The xerogels showed a lamellar structure for $\mathbf{1}_2$ and $\mathbf{1}_4$ and a fiber structure for $\mathbf{1}_3$ and $\mathbf{1}_5$ according to whether the number of methylene units between the two nitrogens was even or odd. The difference in these organogel supramolecular structures has successfully been transcribed into silica structures by sol–gel polymerization of tetraethoxysilane (TEOS) in the gel phase. These results indicate that the novel silica structures can be created by transcription of various superstructures in organogels as a template through hydrogen-bonding interaction. Nitrogen adsorption–desorption isotherms were measured by a BET method. The silica obtained from $\mathbf{1}_2$ and $\mathbf{1}_3$ had a BET surface area of 698 and 525 $m^2\ g^{-1}$, respectively. To deposit metals inside the silica structure, sol–gel polymerization was carried out in the presence of metal salts. The metal ions bound to the diamine moiety were thereby deposited inside the silica wall. It is certain that metal-deposited silica will be applicable as catalysts to various reactions, which require a size recognition ability.

Introduction

The use of organic molecules, assemblies and supramolecular systems in the development of novel inorganic materials continues to offer new and exciting alternatives to conventional synthetic strategies.[1] Since these higher-order aggregates can provide various architectures, utilizing them as templates for sol–gel polymerization results in various novel architectures which cannot be created directly from inorganic materials. As possible templates, proteins, multicellular superstructures, surfactants and DNA have been utilized to create such novel structures of inorganic materials.[2] Recently, the exploitation of new organic gelators which can gelate various organic solvents has become an active area of research.[3–13] These organogels are of particular interest in that they are different from polymer gels, being fibrous aggregates of low molecular-weight compounds formed by non-covalent interactions, responsible for such gelation phenomena. This is why the xerogels can exhibit various superstructures, reflecting the monomeric structure of each gelator. More recently, it was found that certain cholesterol derivatives can gelate even tetraethoxysilane (TEOS), which forms silica gel by sol–gel polymerization.[9,13] Very interestingly, it was shown that sol–gel polymerization of gelated TEOS solutions followed by calcination affords novel silica with a hollow fiber structure because the organogel fibers act as a template to create an inner hollow tube in the polymerization process.[14,15]

The known cholesterol gelators can be classified into two different aggregation modes, one having a fibrous and one having a lamellar structure. To the best of our knowledge, however, there is no general rule for producing fibrous or lamellar aggregates in organogels. We report the first example of these two different aggregation modes being produced by an odd–even effect in ‘gemini’-type cholesterol-based gelators, which can be successfully transcribed into silica by sol–gel polymerization of gelated tetraethoxysilane (TEOS).[16] In addition, it is certain that if gelator-bound metal ions are deposited on the surface of the resultant silica after calcination, the resulting material should be applicable as a novel catalyst to various reactions which require size recognition ability.[17] To realize these intriguing ideas, cholesterol-based gelators ($\mathbf{1}_n$) bearing a cholesterol moiety as an aggregate-forming site and an amine moiety as a metal-binding site were synthesized. We have previously found that the presence of a moderate amount of cationic charge along the template aggregates is indispensable for the template effects to transcribe the organogel structure into silica.[14,15] In addition, Pinnavaia and co-workers[18] recently reported that mesoporous silica is produced by hydrogen-bonding interaction between a diamine surfactant as an organic template and TEOS as an inorganic material in the solution phase. We considered, however, that the organogel phase should be superior to the solution phase, because the organogel fibers formed in the gel phase should be more robust as a template than aggregates formed in the solution phase.[7,9,11] Thus, our

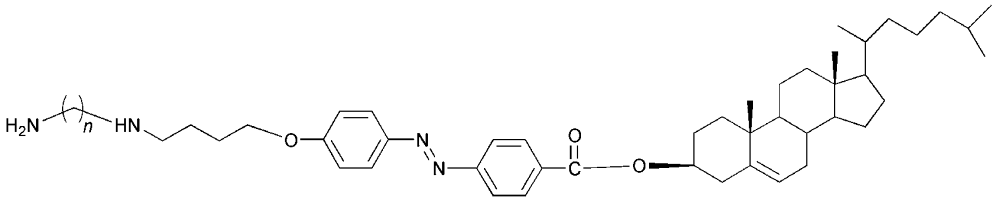

$\mathbf{1}_n = \left(\begin{array}{l} \mathbf{1}_2 : n = 2,\ \mathbf{1}_3 : n = 3 \\ \mathbf{1}_4 : n = 4,\ \mathbf{1}_5 : n = 5 \end{array} \right)$

DOI: 10.1039/b007373n

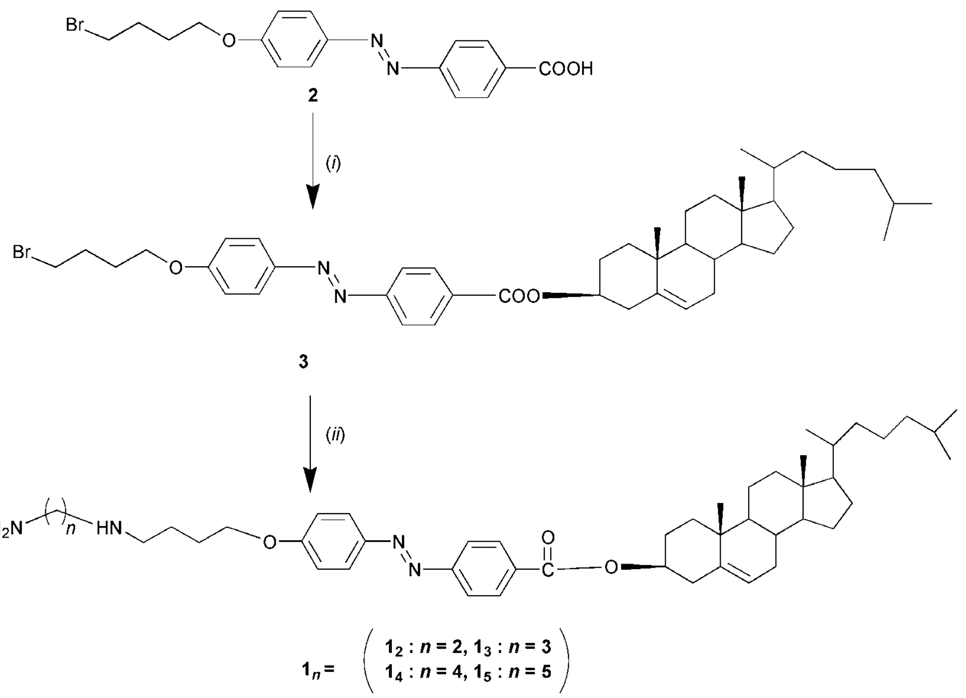

Scheme 1 *Reagents and conditions*: (*i*) cholesterol, DCC, DMAP, dichloromethane, (*ii*) 1,2-diaminoethane, 1,3-diaminopropane, 1,4-diaminobutane or 1,5-diaminopentane, Na_2CO_3, *n*-butyronitrile.

Table 1 Gelation ability of $\mathbf{1}_n$ in organic solvents[a]

	$\mathbf{1}_2$	$\mathbf{1}_3$	$\mathbf{1}_4$	$\mathbf{1}_5$
Methanol	R	R	R	R
Ethanol	R	R	R	R
Propan-1-ol	G	G	G	G
Butan-1-ol	G	G	G	G
Hexan-1-ol	G	G	G	G
THF	S	S	S	S
Acetone	R	R	R	R
Acetonitrile	I	I	I	I
DMSO	G	G	G	G
DMF	G	G	G	G
Aniline	G	G	G	G
Benzene	G	G	G	G
Hexane	R	R	R	R
Acetic acid	R	PG	PG	PG
Dichloromethane	S	S	S	S

[a] Gelator = 5.0 wt%; G = stable gel formed at room temperature; S = solution; I = insoluble; R = recrystallization; PG = partially gelatinized.

initial motivation to prepare cholesterol-based gelators ($\mathbf{1}_n$) was not only to observe the influence of an odd–even effect on the aggregation modes but also to prepare silica with a novel tubular structure through the cationic-charge effect[14,15] and/or the hydrogen-bonding interaction effect[18] operating in the sol–gel transcription processes.

Results and discussion

Gelation ability and SEM observations of xerogels

Compounds $\mathbf{1}_n$ were synthesized according to Scheme 1. The gelation abilities of $\mathbf{1}_n$ were examined in 15 organic solvents. The results are summarized in Table 1. These gelators could gelate 7 out of 15 organic solvents, indicating that they act as versatile gelators of organic solvents. In particular, it is seen from Table 1 that the gelation ability for polar solvents is quite general and excellent.

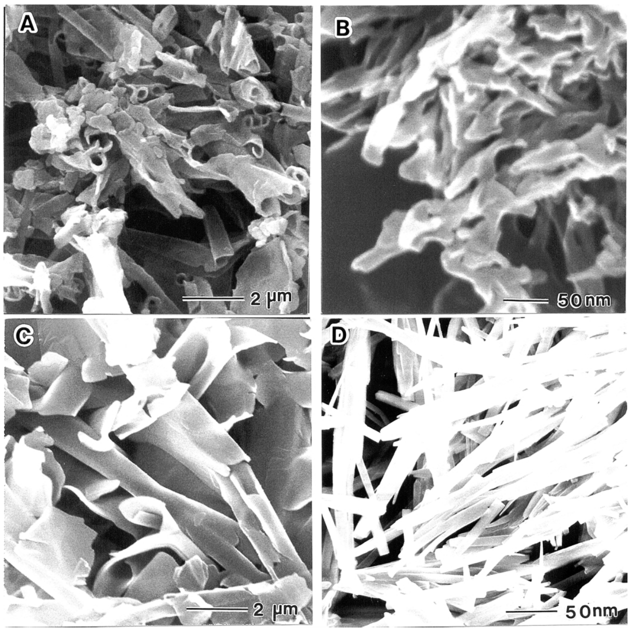

Fig. 1 SEM pictures of xerogels (A) $\mathbf{1}_2$, (B) $\mathbf{1}_3$, (C) $\mathbf{1}_4$ and (D) $\mathbf{1}_5$ obtained from their aniline gels.

To obtain visual insights into the aggregation mode, the superstructures constructed in organogels were observed by SEM. Very surprisingly, the xerogels formed by the four gelators can be classified into two different structures. Compounds $\mathbf{1}_2$ and $\mathbf{1}_4$, which have an even number of methylene units between the NH and NH_2 groups, formed a translucent organogel with aniline. The SEM image did not show a fibrous structure, characteristic of organogel systems but rather featured film-like aggregates of 60–330 nm thickness and a few μm length, which probably consist of lamellar structures (Figs. 1A and 1C). It is noteworthy that some films are curved to form pseudo-cylindrical structures. In contrast, $\mathbf{1}_3$ and $\mathbf{1}_5$, which have an odd number of methylene units between the NH and NH_2 groups, featured fibrous structures with 20–50 and 10–70 nm thickness for $\mathbf{1}_3$ and $\mathbf{1}_5$, respectively (Figs. 1B and 1D). These novel findings prove that the organogel structure is influenced by the number of methylene units between the NH and NH_2 groups. The clear difference between the odd-numbered gelators and the even-numbered gelators implies that the aggregation mode is crucially governed by the molecular packing of

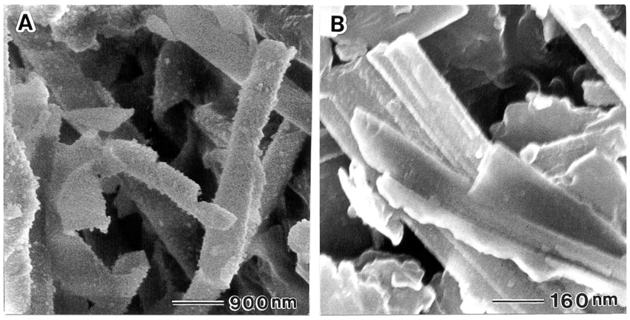

Fig. 2 SEM pictures of the silica obtained from (A) $\mathbf{1}_2$ and (B) $\mathbf{1}_3$ in butan-1-ol before calcination.

the terminal groups. According to Shimizu *et al.*,[19] amide-based bolaamphiphiles with an odd number of methylene units tend to grow as plates or amorphous powder, whereas those with an even number of methylene units tend to grow as fibrous aggregates. The correlation between even/odd and fiber/film (plate) is opposite to the present system. We consider that this disparity is due to a structural difference: Shimizu's system is related to bolaamphiphiles whereas our system is related to the terminal $H_2N(CH_2)_nNH$ gelators.

Sol–gel polymerization towards transcription of the organogel structure

To transcribe the superstructure formed in the organogel into the silica structure, we carried out a sol–gel polymerization of TEOS using $\mathbf{1}_n$ in butan-1-ol according to the method described previously.[14,15] For example, $\mathbf{1}_2$ (5.8×10^{-6} mol) was dissolved in a medium (6.74 g) for sol–gel polymerization: the medium consists of butan-1-ol (or aniline), TEOS, water and benzylamine as a catalyst (see the Experimental section for the details). The sample was sealed in a glass tube and left at ambient temperature for 3–10 days. Subsequently, the sample was heated at 200 °C for 2 h, 500 °C for 2 h under a nitrogen atmosphere and then kept at 500 °C under aerobic conditions for 4 h. We observed the SEM pictures of the silica obtained from $\mathbf{1}_n$ before calcination (Fig. 2). The silica obtained from $\mathbf{1}_2$ space possesses a rolled-paper-like hollow structure arising from the template organogel films, which has an inner diameter of 380–400 nm and a wall thickness of 40–60 nm. On the other hand, the resultant silica obtained from $\mathbf{1}_3$ featured a fibrous structure, which did not appear to be hollow. The contrasting results obtained from $\mathbf{1}_2$ and $\mathbf{1}_3$ suggest that the oligomeric silica species are adsorbed onto these aggregates mainly by the hydrogen-bonding interaction between TEOS and the amino groups of the gelators.[18] After calcination by which the organic compounds are removed through combustion, the morphological structures of the silica were examined in a similar fashion to those before calcination. The silica obtained from $\mathbf{1}_2$ and $\mathbf{1}_4$ shows a rolled-paper-like structure (Figs. 3A and 3C), which is basically similar to that formed in organogels (see Figs. 1A and 1C). On the other hand, the silica obtained from $\mathbf{1}_3$ and $\mathbf{1}_5$ shows a fibrous structure, which has inner and outer diameters of 15–40 and 50–150 nm, respectively (Figs. 3B and 3D). The inner diameters are approximately comparable to those of the organogel fiber diameters (10–70 nm). These results clearly indicate that the organogel structure is finely transcribed into the silica mainly due to the adsorption of oligomeric silica species onto the gelator surface by hydrogen-bonding interaction. The absence of the hollow structure before calcination and the appearance of it after calcination also support this transcription mechanism.

When a trace amount of acid is present in the sol–gel medium, the amino groups are protonated and the cationic charges thus formed can be a driving force to adsorb anionic oligomeric silica particles.[14,15] To obtain evidence for the contribution of the hydrogen-bonding interaction between the 'neutral' amino groups and oligomeric silica particles, sol–gel polymerization was carried out in the presence of Et_4NOH (tetraethylammonium hydroxide: 3 equivalents to $\mathbf{1}_n$), a strong base. As expected, the silica produced under these conditions also showed a tubular structure. These results again support the importance of intermolecular hydrogen-bonding interaction in the creation of hollow fiber silica.[20] In addition, when sol–gel polymerization was carried out in aniline (it is inconceivable that the amino groups are protonated in this basic solvent), the silicas obtained from $\mathbf{1}_4$ and $\mathbf{1}_5$ possessed structures very similar to those obtained in butan-1-ol (lamellar and fibrous, respectively).

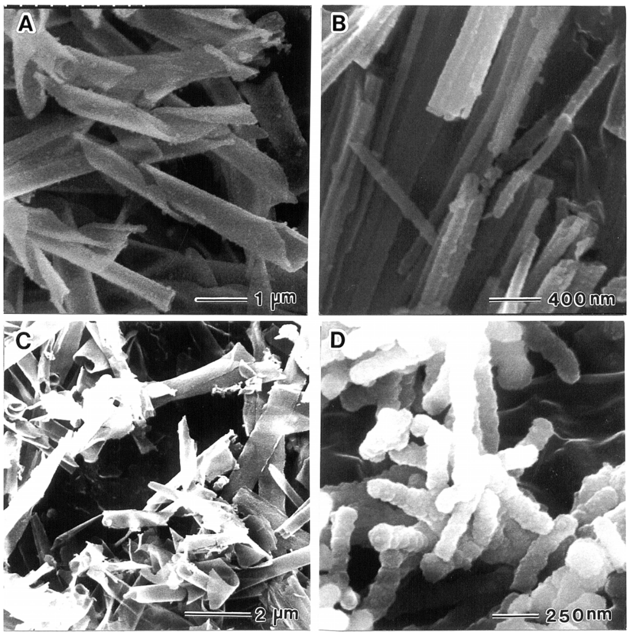

Fig. 3 SEM pictures of the silica obtained from (A) $\mathbf{1}_2$, (B) $\mathbf{1}_3$, (C) $\mathbf{1}_4$ and (D) $\mathbf{1}_5$ in butan-1-ol after calcination.

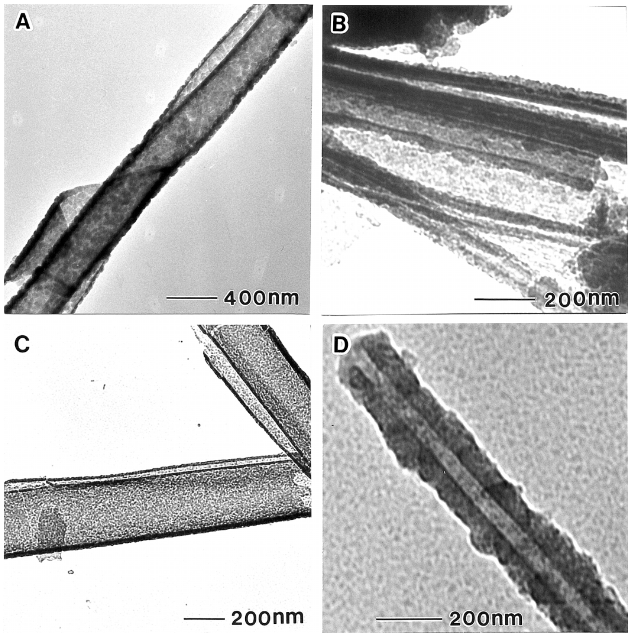

Fig. 4 TEM pictures of the silica obtained from (A) $\mathbf{1}_2$, (B) $\mathbf{1}_3$, (C) $\mathbf{1}_4$ and (D) $\mathbf{1}_5$ in butan-1-ol after calcination.

To further corroborate that the organogel fiber really acted as a template for the growth of the tubular silica, we took TEM pictures after removal of $\mathbf{1}_n$ by calcination. Very interestingly, we found that the silicas had tubular structures with 15–40 nm obtained from $\mathbf{1}_3$ and $\mathbf{1}_5$ and 300–400 nm obtained from $\mathbf{1}_2$ and $\mathbf{1}_4$, respectively (Fig. 4). The results support the view that

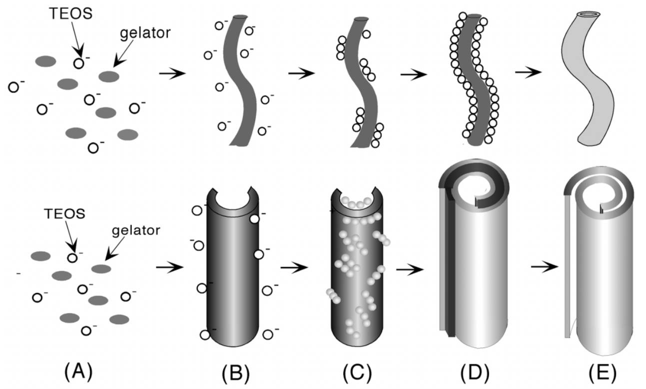

Fig. 5 Schematic representation of the creation of rolled-paper-like silica from the organogel state of $\mathbf{1}_2$ and $\mathbf{1}_4$ (lower) and hollow fiber silica from $\mathbf{1}_3$ and $\mathbf{1}_5$ (upper) by sol–gel polymerization: (A) mixture of gelators and TEOS; (B) gelation; (C) sol–gel polymerization of TEOS and adsorption onto the gelator; (D) before calcination (SEM pictures in Fig. 2 were taken at this stage); (E) rolled-paper-like multi-layer structure (lower) and hollow fiber structure (upper) of the silica formed after calcination (SEM and TEM pictures in Figs. 3 and 4 were taken at this stage).

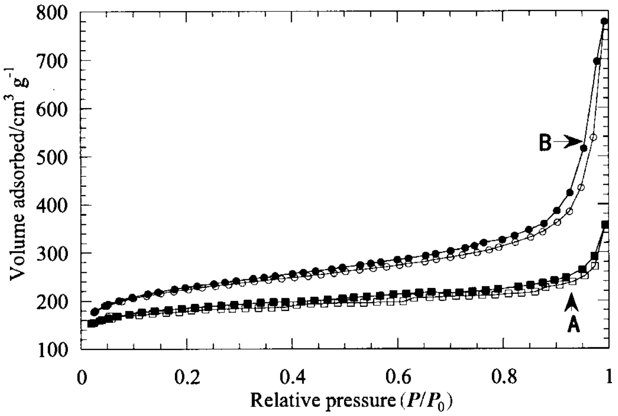

Fig. 6 Nitrogen adsorption–desorption isotherms of the silica obtained from (A) $\mathbf{1}_3$ and (B) $\mathbf{1}_4$.

anionic oligomeric siloxanes are adsorbed onto the neutral organogel fiber by hydrogen-bonding interaction.

As a summary of the foregoing observations, we now propose mechanisms for the formation of novel multi-layered silica from $\mathbf{1}_3$ and $\mathbf{1}_5$ and that of hollow fiber silica from $\mathbf{1}_2$ and $\mathbf{1}_4$ as shown in Fig. 5. Anionic oligomeric silica species are adsorbed onto the surface of the fibrous structure of $\mathbf{1}_3$ or $\mathbf{1}_5$ and the polymerization further proceeds along these fibrils. This propagation mode eventually yields fibrous silica with a tubular structure after combustion of the gelators by calcination (Fig. 5A). In contrast, $\mathbf{1}_2$ or $\mathbf{1}_4$ possesses a curved lamellar structure. Then, the rolled-paper-like silica grows by sol–gel polymerization along this curved surface (Fig. 5B). As supported by a good correlation between the xerogel structures (Fig. 1) and the resultant silica gel structures (Fig. 3), the organogel structures are directly and scrupulously transcribed into the silica utilizing electrostatic and/or hydrogen-bonding interactions.

Nitrogen adsorption–desorption isotherms and deposition of metal particles inside the silica

Representative nitrogen adsorption–desorption isotherms are shown in Fig. 6. The silicas obtained from $\mathbf{1}_2$ and $\mathbf{1}_3$ have a Brunauer–Emmett–Teller (BET) surface area of 699 and 525 $m^2\ g^{-1}$, respectively. The surface area of the silica obtained from $\mathbf{1}_2$ is larger than that of the silica mesophase fiber obtained from the block-copolymer template reported by Stucky *et al.* (580 $m^2\ g^{-1}$).[21]

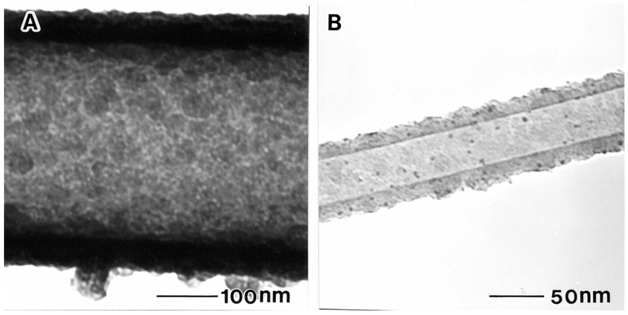

Fig. 7 TEM pictures of the silica obtained from (A) $\mathbf{1}_2\cdot Ni(NO_3)_2$ and (B) $\mathbf{1}_3\cdot Pd(NO_3)_2$ in butan-1-ol after calcination.

It is known that amino groups have a high affinity for transition metals.[22] Particularly, $\mathbf{1}_2$ and $\mathbf{1}_3$ bearing the ethylenediamine skeleton and the propylenediamine skeleton, respectively, should act as good ligands. When sol–gel polymerization of TEOS is carried out in the presence of these metal-binding species, metals could be deposited on the surface of the resulting silica after calcination. With this intriguing idea in mind, sol–gel polymerization of $\mathbf{1}_2$ and $\mathbf{1}_3$ was carried out in the presence of $Ni(NO_3)_2$ and $Pd(NO_3)_2$ respectively. The TEM pictures of the silica thus obtained are shown in Fig. 7. Careful examination of Fig. 7A [$\mathbf{1}_2\cdot Ni(NO_3)_2$ system] reveals that there are many very small dots (<1 nm) of Ni on the silica wall of the rolled-paper-like hollow structure. In the $\mathbf{1}_3\cdot Pd(NO_3)_2$ system, Pd is deposited as larger particles (1–2 nm) inside the silica tube (Fig. 7B). These results support the view that metal salts complexed by gelators are dispersed in the superstructures and, after sol–gel polymerization followed by calcination, are retained in the silica structure. We believe that this metal deposition method is useful for the design of novel solid catalytic systems.

Conclusion

The present paper has clearly demonstrated that the structures of 'gemini'-type organic gelators can be classified into those exhibiting either a lamellar or fibrous structure depending on the number of methylene units between the NH and NH_2 groups. The novel silica structures are created with the aid of hydrogen-bonding interaction of the oligomeric silica species with the gelators. In addition, metals are conveniently deposited inside the silica by metal–ligand interaction. We believe that the present system is not only useful for transcription of various organogel superstructures into silica gel, but also readily applicable to the design of novel solid catalysts featuring a size recognition ability.

Experimental

Equipment

^1H and ^{13}C NMR spectra were measured on a Bruker ARX 300 apparatus. *J* values are given in Hz. IR spectra were obtained from KBr pellets using a Shimadzu FT-IR 8100 spectrometer, and MS spectra were obtained using a Hitachi M-2500 mass spectrometer. Transmission electron microscopy (TEM) was performed on a Hitachi H-7100 at 100 kV. Samples were prepared by adhering a large number of calcined silica particles onto a carbon film on a Cu grid. All reactions were conducted under dry N_2 unless otherwise stated. All reagents were the best grade commercially available ones which were distilled, recrystallized or used with further purification, as appropriate.

SEM measurements

A Hitachi S-14500 scanning electron microscope was used for taking the SEM pictures. The thin gel was prepared in a 1–2 ml bottle and frozen in liquid nitrogen or dry ice–acetone. The frozen specimen was evaporated by a vacuum pump for 24 h. The dry sample was coated with palladium–platinum. The accelerating voltage of the SEM was 5–15 kV and the emission current was 10 μA.

Gelation test of organic fluids

The gelator and the solvent were put in a septum-capped test tube and heated until the solid was dissolved. The solution was cooled at room temperature. If the stable gel was observed at this stage, it was classified as G.

Sol–gel polymerization of TEOS

In a typical preparation a 5.8×10^{-6} mol quantity of gelator was dissolved in butan-1-ol (or aniline) (6.0 g), TEOS (0.45 g), water (0.15 g) and benzylamine (0.14 g: as a catalyst). The mixture was warmed until a transparent solution was obtained. The reaction mixture was placed at room temperature under static conditions for 3–10 days. The product was dried by a vacuum pump at room temperature. Finally, the gelator was removed by calcination at 200 °C for 2 h, 500 °C for 2 h under a nitrogen atmosphere and 500 °C for 4 h under aerobic conditions.

4-Bromobutoxy-4′-[(cholesteryloxy)carbonyl]azobenzene (3)

4-[(4-Bromobutoxyphenyl)azo]benzoic acid **2** (0.7 g, 1.86 mmol) and cholesterol (0.718 g, 2.23 mmol) were dissolved in 20 ml of dichloromethane under a nitrogen atmosphere. The solution was maintained at 0 °C using an ice bath. The dicyclohexylcarbodiimide (DCC) (0.383 g, 1.86 mmol) and *N*,*N*-dimethylaminopyridine (DMAP) (0.022 g, 0.186 mmol) were then added, the reaction mixture being stirred for 4 h at 0 °C. The reaction mixture was filtered and the filtrate was washed with acidic and basic aqueous solutions (50 ml each). The organic layer was evaporated to dryness. The residue was purified by a silica-gel column eluting with THF–*n*-hexane (1 : 6 v/v) to give compound **3** in 26% yield as a yellow solid (mp 141.5 °C). ^{1}H NMR (300 MHz, $CDCl_3$): δ_H 8.17 (2H, d, $J = 9.0$), 7.72 (2H, d, $J = 9.0$), 7.90 (2H, d, $J = 9.0$), 7.10 (2H, d, $J = 9.0$), 5.45 (1H, d, $J = 6.3$), 5.02–4.88 (1H, m), 4.10 (2H, t, $J = 6.3$), 3.52 (2H, t, $J = 6.2$), 2.49 (2H, d, $J = 6.2$), 2.28–0.94 (35H, m), 0.88 (3H, s); ^{13}C NMR (75 MHz, $CDCl_3$): δ_C 165.1, 161.88, 155.20, 146.98, 139.9, 130.2, 125.18, 122.84, 122.28, 114.72, 67.22, 66.67, 56.67, 56.11, 50.01, 42.30, 39.71, 39.50, 38.20, 37.01, 36.64, 36.17, 35.79, 33.32, 31.92, 31.86, 29.3, 28.32, 28.01, 27.88, 27.78, 24.28, 23.82, 22.83, 22.56, 21.04, 19.38, 19.38, 18.71, 11.86; MS (*m*/*z*) 745 $[M + H]^+$; IR (KBr, ν_{max}/cm^{-1}): 3005 (Ar), 2935 (–CH), 1722 (–C=O), 1603, 1579, 1500, 1468 (Ar), 1284, 1116, 1047 (–C–O).

4-(2-Aminoethylamino)butoxy-4′-[(cholesteryloxy)carbonyl]-azobenzene (1_2)

A mixture of compound **3** (0.05 g, 0.067 mmol), 1,2-diaminoethane (0.04 g, 0.67 mmol), and sodium carbonate (0.3 g, 6.7 mmol) in dry *n*-butyronitrile (10 ml) was refluxed for 24 h. The solution was filtered after cooling, the filtrate being concentrated to dryness by a vacuum evaporator. The residue was purified by an aluminium oxide column with ethanol–dichloromethane to give the desired product in 43.3% yield as a yellow solid (mp 129–131.1 °C). ^{1}H NMR (300 MHz, $CDCl_3$): δ_H 8.17 (2H, d, $J = 9.1$), 7.93 (2H, d, $J = 9.1$), 7.88 (2H, d, $J = 9.0$), 7.01 (2H, d, $J = 9.0$), 5.45 (1H, d, $J = 6.5$), 4.75 (1H, m), 3.6–3.4 (6H, m), 2.78 (4H, t, $J = 12.1$), 2.75 (2H, t, $J = 6.5$), 2.49 (2H, d, $J = 6.3$), 2.25–0.69 (44H, m); MS (*m*/*z*) 726 $[M + 2H]^+$; IR (KBr, ν_{max}/cm^{-1}): 3005 (Ar), 2943 (–CH), 2868, 1711 (–C=O), 1599, 1581, 1500, 1468, 1419 (Ar), 1404, 1275, 1140, 1109 (–C–O). Anal. Calcd for $C_{46}H_{68}N_4O_3$: C, 73.27; H, 9.45; N, 7.72. Found: C, 73.27; H, 9.45; N, 7.95%.

4-(3-Aminopropylamino)butoxy-4′-[(cholesteryloxy)carbonyl]-azobenzene (1_3)

The method described above for the synthesis of $\mathbf{1_2}$ was followed, and the title compound was obtained in 25.0% yield as a yellow solid (mp 135.5–136.0 °C). ^{1}H NMR (300 MHz, $CDCl_3$): δ_H 8.17 (2H, d, $J = 9.0$), 7.93 (2H, d, $J = 9.0$), 7.88 (2H, d, $J = 9.0$), 7.01 (2H, d, $J = 9.0$), 5.45 (1H, d, $J = 6.5$), 4.75 (1H, m), 3.6–3.4 (6H, m), 2.78 (4H, t, $J = 12.1$), 2.75 (2H, t, $J = 6.5$), 2.49 (2H, d, $J = 6.3$), 2.30–0.69 (46H, m); MS (*m*/*z*) 740.08 $[M + H]^+$; IR (KBr, ν_{max}/cm^{-1}): 3005 (Ar), 2937 (–CH), 1722 (–C=O), 1603, 1579, 1500, 1468 (Ar), 1284, 1116, 1047 (–C–O). Anal. Calcd for $C_{47}H_{70}N_4O_3$: C, 76.38; H, 9.55; N, 7.75. Found: C, 75.55; H, 9.28; N, 7.50%.

4-(4-Aminobutylamino)butoxy-4′-[(cholesteryloxy)carbonyl]-azobenzene (1_4)

The method described above for the synthesis of $\mathbf{1_2}$ was followed, and the title compound was obtained in 52.5% yield as a yellow solid (mp 132.7–133.5 °C). ^{1}H NMR (300 MHz, $CDCl_3$): δ_H 8.17 (2H, d, $J = 9.0$), 7.93 (2H, d, $J = 9.0$), 7.88 (2H, d, $J = 9.0$), 7.01 (2H, d, $J = 9.0$), 5.50 (1H, d, $J = 6.5$), 4.80 (1H, m), 3.6–3.4 (6H, m), 2.78 (4H, t, $J = 12.1$), 2.75 (2H, t, $J = 6.5$), 2.49 (2H, d, $J = 6.3$), 2.35–0.69 (48H, m); MS (*m*/*z*) 754 $[M + H]^+$; IR (KBr, ν_{max}/cm^{-1}): 3005 (Ar), 2935 (–CH), 1722 (–C=O), 1603, 1579, 1500, 1468 (Ar), 1284, 1116, 1047 (–C–O–). Anal. Calcd for $C_{48}H_{72}N_4O_3$: C, 76.55; H, 9.64; N, 7.44. Found: C, 76.05; H, 9.50; N, 7.50%.

4-(5-Aminopentylamino)butoxy-4′-[(cholesteryloxy)carbonyl]-azobenzene (1_5)

The method described above for the synthesis of $\mathbf{1_2}$ was followed, and the title compound was obtained in 45.0% yield as a yellow solid (mp 128.7–129.5 °C). ^{1}H NMR (300 MHz, $CDCl_3$): δ_H 8.17 (2H, d, $J = 9.0$), 7.93 (2H, d, $J = 9.0$), 7.88 (2H, d, $J = 9.0$), 7.01 (2H, d, $J = 9.0$), 5.48 (1H, d, $J = 6.5$), 4.78 (1H, m), 3.6–3.4 (6H, m), 2.78 (4H, t, $J = 12.1$), 2.75 (2H, t, $J = 6.5$), 2.49 (2H, d, $J = 6.3$), 2.35–0.69 (49H, m); MS (*m*/*z*) 769 $[M + H]^+$; IR (KBr, ν_{max}/cm^{-1}): 3005 (Ar), 2935 (–CH), 1722 (–C=O), 1603, 1579, 1500, 1468 (Ar), 1284, 1116, 1047 (–C–O). Anal. Calcd for $C_{49}H_{74}N_4O_3$: C, 76.72; H, 9.72; N, 7.30. Found: C, 76.80; H, 9.73; N, 7.53%.

References and notes

1 S. Mann, *Biomimetic Materials Chemistry*, ed. S. Mann, VCH, New York, 1996.

2 W. Shenton, T. Douglas, M. Young, G. Stubbs and S. Mann, *Adv. Mater.*, 1999, **11**, 253; T. Douglas and M. Young, *Nature*, 1998, **393**, 152; W. Shenton, D. Pum, U. Sleytr and S. Mann, *Nature*, 1997, **389**, 585; S. A. Davis, S. L. Burkett, N. H. Mendelson and S. Mann, *Nature*, 1997, **385**, 420; Y. Ono, Y. Kanekiyo, K. Inoue, J. Hojo, M. Nango and S. Shinkai, *Chem. Lett.*, 1999, 475.

3 J. de Vries and R. M. Kellogg, *J. Chem. Soc.*, *Chem. Commun.*, 1993, 238; M. de Loos, J. van Esch, I. Stokroos, R. M. Kellogg and B. L. Feringa, *J. Am. Chem. Soc.*, 1997, **119**, 12675.

4 M. Aoki, K. Nakasima, H. Kawabata, S. Tsutsui and S. Shinkai, *J. Chem. Soc.*, *Perkin Trans. 2*, 1993, 347.

5 K. Hanabusa, K. Okui, K. Karaki, T. Koyoma and H. Shirai, *J. Chem. Soc.*, *Chem. Commun.*, 1992, 1371; K. Hanabusa, A. Kawakami, M. Kimura and H. Shirai, *Chem. Lett.*, 1997, 191 and references cited therein.

6 J.-E. Sohna Sohna and F. Fages, *Chem. Commun.*, 1997, 327.

7 E. Ostuni, P. Kamaras and R. G. Weiss, *Angew. Chem.*, *Int. Ed. Engl.*, 1996, **35**, 1324 and references cited therein.

8 P. Terech, I. Furman and R. G. Weiss, *J. Phys. Chem.*, 1995, **99**, 9558 and references cited therein.

9 K. Murata, M. Aoki, T. Suzuki, T. Harada, H. Kawabata, T. Komori, F. Ohseto, K. Ueda and S. Shinkai, *J. Am. Chem. Soc.*, 1994, **116**, 6664 and references cited therein.

10 T. D. James, K. Murata, T. Harada, K. Ueda and S. Shinkai, *Chem. Lett.*, 1994, 273.

11 S. W. Jeong, K. Murata and S. Shinkai, *Supramol. Sci.*, 1996, **3**, 83.

12 T. Brotin. R. Utermöhlen, F. Fages, H. Bouas-Laurent and J.-P. Desvergne, *J. Chem. Soc.*, *Chem. Commun.*, 1991, 416.

13 For recent comprehensive reviews, see P. Terech and R. G. Weiss, *Chem. Rev.*, 1997, 3133; S. Shinkai and K. Murata, *J. Mater. Chem.*, 1998, **8**, 485.

14 Y. Ono, K. Nakashima, M. Sano, Y. Kanekiyo, K. Inoue, J. Hojo and S. Shinkai, *Chem. Commun.*, 1998, 1477.

15 Y. Ono, Y. Kanekiyo, K. Inoue, J. Hojo and S. Shinkai, *Chem. Lett.*, 1999, 23; J. H. Jung, Y. Ono and S. Shinkai, *Langmuir*, 2000, **16**, 1643; J. H. Jung, Y. Ono and S. Shinkai, *Angew. Chem.*, *Int. Ed.*, 2000, **39**, 1862; J. H. Jung, Y. Ono and S. Shinkai, *J. Chem. Soc.*, *Perkin Trans. 2*, 1999, 1289; G. M. Clavier, J. L. Pozzo, H. Bouas-Laurent, C. Liere and C. Sanchez, *J. Mater. Chem.*, 2000, **10**, 1725.

16 Preliminary communication: J. H. Jung, Y. Ono and S. Shinkai, *Chem. Lett.*, 2000, 636.

17 J. Y. Ying, C. P. Mehnert and M. S. Wong, *Angew. Chem.*, *Int. Ed.*, 1999, **38**, 56; C. P. Mehnert and J. Y. Ying, *Chem. Commun.*, 1997, 2215; C. P. Mehnert, D. W. Weaver and J. Y. Ying, *J. Am. Chem. Soc.*, 1998, **120**, 12289.

18 S. S. Kim, W. Zhang and T. J. Pinnavaia, *Science*, 1998, **282**, 1302; P. T. Tanev, Y. Liang and T. J. Pinnavaia, *J. Am. Chem. Soc.*, 1997, **119**, 8616.

19 M. Masuda, T. Habada, K. Yaso and T. Shimizu, *Macromolecules*, 1998, **31**, 9403; T. Shimizu and M. Masuda, *J. Am. Chem. Soc.*, 1997, **119**, 2812; M. Kogiso, T. Hanada, K. Yaso and T. Shimizu, *Chem. Commun.*, 1998, 1791; M. Kogiso, M. Masuda and T. Shimizu, *Supramol. Chem.*, 1998, **9**, 183.

20 We previously synthesized cholesterol-based gelators bearing the monoaza-18-crown-6 moiety (compound A) and diaza-18-crown-6 (compound B). Compound A induced the granular silica structure in the presence of Et_4NOH. In contrast, compound B still yielded the hollow fiber silica even in the presence of Et_4NOH. These results indicate that –NH is indispensable for efficient interaction between gelators and oligomeric silica particles.

21 P. Yang, D. Zhao, B. F. Hmelka and G. D. Stucky, *Chem. Mater.*, 1998, **10**, 2033.

22 R. M. Izatt, K. Pawlak and J. S. Bradshow, *Chem. Rev.*, 1995, **95**, 2529.